Supplementary material:

CFD modelling and experimental analysis of aromatic amine extraction in a flat sheet supported liquid membrane contactor

Gilles Van Eygen[a,b,c,*], Emma Lodewijckx[a], Sean Van Gestel[a], Nilay Baylan[a,d], Anita Buekenhoudt[c], João A.P. Coutinho[e], Bart Van der Bruggen[a], Patricia Luis[b,f]

a Process Engineering for Sustainable Systems (ProcESS), KU Leuven, Celestijnenlaan 200f, 3001 Leuven (Belgium)

b Materials & Process Engineering (IMAP), UCLouvain, Place Sainte Barbe 2, B-1348 Louvain-la-Neuve (Belgium)

c Unit Separation and Conversion Technology, Vlaamse Instelling voor Technologisch Onderzoek (VITO NV), Boeretang 200, 2400 Mol (Belgium)

d Department of Chemical Engineering, Istanbul University-Cerrahpaşa, Avcılar, 34320, Istanbul, Turkey

e CICECO-Aveiro Institute of Materials, Chemistry Department, University of Aveiro, 3810-193 Aveiro, Portugal

f Research & Innovation Centre for Process Engineering (ReCIPE), Place Sainte Barbe 2, bte L5.02.02, B-1348 Louvain-la-Neuve (Belgium), Tel: +32 (0)10 47 25 87 - Fax: +32(0)10 47 40 28

* Corresponding author: gilles.vaneygen@vito.be

Keywords — Ionic liquids, supported liquid membranes, extraction, computational fluid dynamics.

S1 Buffer preparation

Table S1. Composition of the used feed buffers for a volume of 500 mL Milli-Q water.

pH [-]	$m(NaHCO_3)$ [g]	$m(Na_2CO_3)$ [g]	$m(NaH_2PO_4)$ [g]	$V(H_3PO_4)$ [µL]
3.0	0	0	10.49	862
9.0	60	3.7	0	0
9.5	35	6.8	0	0
10.0	25	15.1	0	0
10.5	15	29.3	0	0
11.0	6.5	40	0	0

S2 Solvent usage

The solvent usage was quantified as the mass of ionic liquid impregnated into the membrane pores (m_{IL}), calculated using the following equation:

$$m_{\mathrm{IL}}(\mathrm{g}) = m_{\mathrm{wet}} - m_{\mathrm{dry}} \tag{1}$$

where m_{wet} and m_{dry} are the wet and dry membrane mass, respectively. The impregnation efficiency (IE_{IL}) of the membrane was calculated as:

$$IE_{\mathrm{IL}}\left(\frac{\mathrm{g}}{\mathrm{m}^2}\right) = \frac{m_{\mathrm{IL}}}{A_{\mathrm{tot}}} = \frac{m_{\mathrm{wet}}-m_{\mathrm{dry}}}{\pi R^2} \tag{2}$$

where A_{tot} is the total membrane surface used for impregnation, and R = 23 mm is the radius of the membrane. The solvent-to-feed ratio (SF) was determined as:

$$SF\left(\frac{\mathrm{kg_{IL}}}{\mathrm{kg_{feed}}}\right) = \frac{m_{\mathrm{IL}}}{m_{\mathrm{feed}}} \tag{3}$$

in which m_{feed}, the total feed solution used for each experiment, was approximately 500 g. Table S2 shows that less than 40 g/m² of ionic liquid is required to impregnate the membrane. Additionally, the solvent-to-feed ratio remained below $2.0 \cdot 10^{-4}$ kg of ionic liquid per kg of feed solution across all tested conditions (see Figure S1). In contrast, conventional LLE typically employs significantly higher solvent-to-feed ratios, such as 1.5 for achieving 98-99% extraction of acetic acid, 3.5–5 for removing acids at concentrations below 1000 ppm from wastewater, and 0.2 for extraction of phenol at concentrations below 50 ppm [1].

Table S2. Impregnation efficiency of the membrane (IE_{IL}) expressed as grams of ionic liquid per square meter of membrane surface, across all tested conditions. The mass of ionic liquid (m_{IL}) impregnated in the SLM, in grams, is also provided for each experiment.

		m^1_{IL}	m^2_{IL}	m^3_{IL}	m^4_{IL}	IE_{IL}
		g	g	g	g	g/m²
F [L/h]	5	0.04443	0.03365	0.06497		28.7 ± 9.6
	7.5	0.04200	0.07771			36.0 ± 15.2
	10	0.01857	0.04822			20.1 ± 12.6
C [g/L]	0.5	0.06124	0.05172			34.0 ± 4.1
	1	0.01857	0.04822			20.1 ± 12.6
	2.5	0.03972	0.05221			27.7 ± 5.3
pH [-]	9	0.05536	0.03637	0.02700	0.03917	23.8 ± 7.1
	9.5	0.03841	0.03224			21.3 ± 2.6
	10	0.01857	0.04822			20.1 ± 12.6
	10.5	0.04098	0.0379			23.7 ± 1.3
	11	0.04488	0.04101	0.03713		24.7 ± 2.3

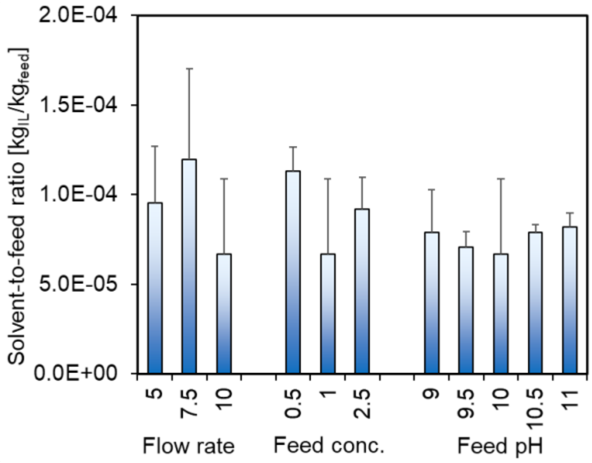

Figure S1. Solvent-to-feed ratio, expressed as kilograms of ionic liquid used per kilogram of feed solution, presented for all experimental conditions.

S3. Model definition

S3.1 Flat sheet module building in Solid Edge

The spiral flat sheet geometry consists of various parts. The most complex part is the spiral itself. This geometry was imported from Solid Edge in which a moat with a diameter and depth of 2 mm was spiralled five times with a 1 mm wall in between moats. The complete spiral had a diameter of 36 mm. The tubing connecting this spiral within the flat sheet module was recreated in COMSOL using cylinders with a diameter of 2 mm. The assumption was made that all surfaces are smooth with rounded bends to overcome narrow regions that would later be unable to create a mesh. Specifically, vertical tubes with a length of 8 mm were connected to quarter tori with major radii of 2 mm, minor radii of 1 mm, and revolution angles of 90 degrees. These tori were further connected to horizontal tubes of 8 mm for the outer connection and 23 mm for the inner connection. Some refinement of the colliding surfaces was used to prevent future mesh problems. The created spiral was then mirrored and a membrane with a thickness of 180 µm was placed in between.

S3.2 Pre-processing

S3.2.1 Defined materials

Within the COMSOL simulation, three different materials were defined. First, the built-in material "Water, liquid" was used to approximate the parameters of both buffer domains. A solid material was user-defined to act as the porous PTFE support in the membrane domain with porosity ϵ = 0.67 and Darcy's permeability κ = 0.06326 D. The permeability is unknown and initially approximated by that of a PVDF/MAF-4 membrane at 0.06326 D [2]. As the permeability is only used to calculate the transmembrane pressure (TMP), which is negligible over an SLM, its effect was neglected. Finally, the extractant phase in the porous support was user-defined, but not allocated to any domain. The extractant of choice for the standard model was the ionic liquid trihexyltetradecylphosphonium bis(trifluoromethylsulfonyl)imide ($[P_{6,6,6,14}][N(Tf)_2]$), which has a dynamic viscosity η of 297.5 mPa s and a density ρ of 1067.9 kg/m^3 [3].

S3.2.2 Buffer reactions

The tested module contains two buffer solutions, namely an alkaline buffer on a carbonate basis (Na_2CO_3 and $NaHCO_3$) and an acidic buffer on a phosphate basis (H_3PO_4, NaH_2PO_4, and Na_2HPO_4). The amines of interest, namely α-methylbenzylamine (MBA), 1-methyl-3-phenylpropylamine (MPPA), and isopropyl amine (IPA) are all defined as a diluted species in the buffer solutions. The pKa values of the different amines are given in Table S3.

Table S3. The pKa values of the considered compounds.

Compound	pKa [-]	References
MBA	9.4 ± 0.35	[4–6]
MPPA	10.0 ± 0.35	[4]
IPA	10.6 ± 0.04	[7]

To calculate the necessary masses (or volume of the 85% w/v H_3PO_4 solution) for the preparation of the various buffers at a chosen pH and buffer capacity, a MATLAB script was written. Additionally, the equilibrium ratio of protonated to unprotonated amines for a given pH could be calculated automatically with the MATLAB script such that this equilibrium could be used as input for the COMSOL model. The script utilises the K_a values which can be found in Table S4. The MATLAB script can be found in Section S4.1 in the Supplementary Material. It is assumed that the addition of amines and buffer compounds has a negligible effect on the parameters of water. Furthermore, it was assumed that a buffer capacity of 0.2 M remained after the addition of amines and their primary formed equilibrium took place. This remaining capacity was assumed to be sufficient to handle all the (de)protonation reactions which occurred in the medium.

Table S4. The K_a values of the buffer compounds, retrieved from Smets et al. [8].

Compound	K_a [mol/L]
H_2CO_3	$4.16 \cdot 10^{-7}$
HCO_3^-	$4.84 \cdot 10^{-11}$
H_3PO_4	$7.5 \cdot 10^{-3}$
$H_2PO_4^-$	$6.2 \cdot 10^{-8}$
HPO_4^{2-}	$1.0 \cdot 10^{-12}$

All the considered buffer reactions and their equilibrium constants are given in Table S5 and Table S6, for the alkaline and acidic buffer domain, respectively. All the introduced reactions had a correction factor c_0 = 1000, which corrected the change in units, as the used K_a to calculate K_{eq} were expressed in mol/L and c_i was represented in mol/m³ within COMSOL. The equilibrium constant K_{eq} was calculated as shown in Equation (4) with ν_i the stoichiometric coefficient, which is defined as positive for products and negative for reagents.

$$K_{eq} = \prod \left(\frac{c_i}{c_0}\right)^{\nu_i} \tag{4}$$

To increase the accuracy, all alkaline domain reactions were chosen to be hydroxide based, while all acidic domain reactions were hydroxonium based. For the same reason, water was neglected in all reactions and was considered abundant.

Table S5. Reactions in the alkaline buffer domain and their respective equilibrium constant K_{eq} [8].

Alkaline domain reactions	K_{eq} [mol/L]
$CO_3^{2-} + H_2O \rightleftharpoons HCO_3^- + OH^-$	$\frac{K_w}{K_a} = \frac{10^{-14}}{4.84 \cdot 10^{-11}}$
$HCO_3^- + H_2O \rightleftharpoons H_2CO_3 + OH^-$	$\frac{K_w}{K_a} = \frac{10^{-14}}{4.16 \cdot 10^{-7}}$
$MBAH^+ + OH^- \rightleftharpoons MBA + H_2O$	$\frac{10^{-pKa}}{K_w} = \frac{10^{-9.4}}{10^{-14}}$
$MPPAH^+ + OH^- \rightleftharpoons MPPA + H_2O$	$\frac{10^{-pKa}}{K_w} = \frac{10^{-10.0}}{10^{-14}}$
$IPAH^+ + OH^- \rightleftharpoons IPA + H_2O$	$\frac{10^{-pKa}}{K_w} = \frac{10^{-10.6}}{10^{-14}}$

Table S6. Reactions in the acidic buffer domain and their respective equilibrium constant K_{eq} [8].

Acidic domain reactions	K_{eq} [mol/L]
$H_3PO_4 + H_2O \rightleftharpoons H_2PO_4^- + H_3O^+$	$K_a = 7.5 \cdot 10^{-3}$
$H_2PO_4^- + H_2O \rightleftharpoons HPO_4^{2-} + H_3O^+$	$K_a = 6.2 \cdot 10^{-8}$
$HPO_4^{2-} + H_2O \rightleftharpoons PO_4^{3-} + H_3O^+$	$K_a = 1.0 \cdot 10^{-12}$
$MBA + H_3O^+ \rightleftharpoons MBAH^+ + H_2O$	$\frac{1}{10^{-pKa}} = \frac{1}{10^{-9.4}}$
$MPPA + H_3O^+ \rightleftharpoons MPPAH^+ + H_2O$	$\frac{1}{10^{-pKa}} = \frac{1}{10^{-10.0}}$
$IPA + H_3O^+ \rightleftharpoons IPAH^+ + H_2O$	$\frac{1}{10^{-pKa}} = \frac{1}{10^{-10.6}}$

S3.2.3 Multiphysics model

As the main physics in which all mass transport and reactions occur, the "Transport of Diluted Species in Porous Media" physics module was used. Unlike its counterpart "Reacting Flow of Diluted Species in Porous Media", this model allows for the modification of the velocity profiles by other physics. More specifically, nonconservative convection was used as additional transport mechanism and fifteen concentration variables were introduced.

For the membrane domain, the "Darcy's Law" physics was used to create a velocity field in the porous PTFE membrane filled with $[P_{6,6,6,14}][N(Tf)_2]$ as the fluid material. It was assumed that there were no gravity effects and an initial condition of 1 bar was chosen. The diffusion coefficients D_i for all components i were set to zero, except for the unprotonated amines MBA, MPPA, and IPA. As their diffusion coefficients were unknown, three pseudo-compounds were defined with pKa values of 9.4, 10.0, and 10.6, each assigned an initial diffusion coefficient of $2.5 \cdot 10^{-10}$ m^2/s. The effective diffusivity was calculated using the saturated Millington and Quirk model such that the tortuosity was calculated as $\tau = \epsilon^{-1/3}$. For a porosity ϵ of 0.67, this gives a tortuosity of

1.14 which is in good agreement with literature values for the tortuosity of PTFE membranes (≈ 1.1) [9,10]. The effective diffusivity $D_{\mathrm{e,a}}$ could then be calculated as follows [11,12]:

$$D_{\mathrm{e,a}} = \frac{\epsilon}{\tau} D_{\mathrm{a}} \tag{5}$$

For the buffer domains, the “Turbulent Flow” physics was used to create a velocity field in the bulk liquid phases. This module makes use of the incompressible RANS $k - \epsilon$ model (with the standard parameter values as defined by COMSOL). Additionally, the domain condition "Transport Properties Liquids" had been added. Herein, the turbulent velocity field was selected and the diffusion coefficients in water were set to 10^{-10} m^2/s for all compounds under the assumption that convection would do most mass transport in the liquid.

Additionally, the boundary condition inflow and outflow were used to create mass transport. The inflow and initial conditions of the feed and stripping side were specified using a MATLAB script (see Section S4.1) to determine both buffer and amine equilibrium concentrations. By using the equilibrium values, the computational time was reduced as the inflow boundaries were already close to their final value. For the standard model, pH values of 10 and 3 were used for the feed and strip side, respectively. Finally, the buffer reactions as shown in Section S3.2.2 were introduced. Furthermore, boundary conditions were added to the inlet and outlet. For the inlet, a normal inflow velocity was used and calculated from the tested volumetric flow rate. For the standard model, the required velocity was calculated as follows:

$$u_0 = \frac{F}{A} = \frac{F}{\pi R^2} = 0.88\ \mathrm{m/s} \tag{6}$$

with F = 10 L/h and R = 1 mm the radius of the inlet tubing of the flat sheet cell. As outlet condition, a pressure of 1 bar with suppressed backflow was applied. To speed up convergence, an initial pressure of 1 bar was assumed as starting point.

S3.2.4 Mesh creation

The coarseness of the mesh affects both the preciseness and computational power. Therefore, a trade-off was required. For the complex spiral geometry, a user-defined mesh was created, which could describe the entire geometry, remained within the memory limit for further LU factorisation, converged within a reasonable time frame, and gave accurate results.

The following procedure was used for the mesh creation. First, all the studied domains were given a free tetrahedral mesh with unidirectional scaling. The tetrahedral mesh size was smoothed over four iterations with a maximum element process depth of four. For the buffer domains, a standard-sized mesh calibrated for fluid dynamics was used, whereas all boundaries of these domains were sized with a fine fluid dynamics mesh. The remaining elements were given a normal sized mesh for general physics. The corners of the buffer domains were then refined for all boundaries, except for the inlets and outlets, with a scaling factor of 0.35 and a minimum boundary angle of 240 degrees. To finish off the mesh, the buffer domains were given boundary layers which had been transitioned from the standard mesh over four smoothing iterations with a maximum element process depth of six. Sharp edges were trimmed between 240 degrees and 40 degrees. A maximum layer decrement, *i.e.*, the maximal difference between the number of boundary layers with neighbouring points, was set to 2. For the boundary elements of these buffer domains, except for the inlets and outlets, two boundary layers had been created with a stretching factor of 1.2 and a thickness adjustment factor of 3. The first layer's thickness was automatically chosen by COMSOL. This final mesh is shown in Figure S2. For the spiral geometry, this resulted in 227,629 domain elements and 31,714 boundary elements in which the physics equations are solved.

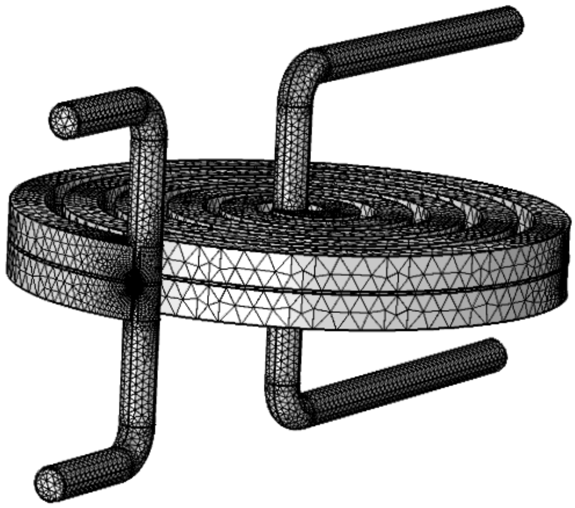

Figure S2. Tetrahedral mesh of 227,629 domain elements generated on the spiral flat sheet module, created in COMSOL.

S3.2.5 Description of the study and the used solver

The final step in the pre-processing stage was the determination of the processing algorithm of the simulation. In COMSOL, this is done by selecting a study and configuring its solver. The multiphysics model of 43 variables was solved as a stationary system within the predetermined mesh. The stationary solver was given a relative tolerance of 10^{-3} with automatic linearity to detect whether the system could be approached linearly. The reaction forces were outputted, but no lumping was used due to the complex 3D geometry [11,12]. Running this solver on the earlier described mesh gave a complexity – described in degrees of freedom (DOFs) solved for – of 1,701,047 DOF and 378,780 internal DOFs.

The chosen solver algorithm was the PARDISO solver using nested multithreaded dissection with an automatic scheduling method. The rows were preordered and the Bunch-Kaufmann 2x2 pivoting was used with a minimum pivot size – denoted as pivoting perturbation – of 10^{-8}. The forwards and backwards solvers were run multithreaded to fully use the cores of the computer for faster solving when iterating. This iterating was still required, despite the use of a direct solver, as the problem had been split into segregated steps to prevent the LU factorisation from running out of memory and to speed up the computation. An automatic error estimation with a standard factor was used [11,12].

Each of the segregated steps made use of a constant Newton nonlinear method with a Jacobian update on each iteration with one segregated iteration per total iteration and solved with the direct solver. The 43 variables were split over five segregated steps. All kinetic variables (velocity, pressures, and turbulence parameters) were bundled with a damping factor of 0.5. The second step contained all the alkaline buffer concentrations, including hydroxide, the alkaline equilibrium reaction rates, and its equilibrium concentration shifts. The third step had these same aspects, but for the acidic buffer and contained hydroxonium ions instead of hydroxide ions. Finally, each amine had its own segregated step containing its deprotonated and protonated concentrations and the reaction rate and shift from both buffers. All non-kinetic steps were given a damping factor of 1 [11,12].

The overall segregated step solver converged if its tolerance was met, with a tolerance factor of 1. The algorithm terminated if a solution was found or gave an error if the residual grew too large, with a factor of 1000. For the pseudo time-stepping, the COMSOL standard values were used. An initial CFL number of 3 was used in combination with a PID regulator in which the proportional factor (P) was 0.65 and both the derivative (D) and integrative (I) factors were 0.05. It had a target error estimate of 0.1 [11,12]. Finally, a lower limit had been implemented in the segregated steps such that no concentration or turbulence parameter could give negative values as a result.

S3.3 Processing

S3.3.1 Single pass analysis

First, the simulations were performed on a single pass through the module. The inlet and outlet concentrations of $\mathrm{OH^-}$, $\mathrm{H_3O^+}$, and the three different amines at both the feed and strip side were obtained from the COMSOL model. This enabled a validation of the buffer pH, both $\mathrm{OH^-}$-based and $\mathrm{H_3O^+}$-based. Furthermore, the molar flow rate $\dot{n}_\mathrm{a}$ [mol/h] of each amine a could be calculated as shown in Equation (7):

$$\dot{n}_\mathrm{a} = Q \cdot (C_\mathrm{a} + C_\mathrm{aH+}) \tag{7}$$

where Q [m³/h] represents the flow rate on the feed side and C_a and $C_\mathrm{aH+}$ [mol/m³] represent the deprotonated and protonated amine concentration, respectively. The two main parameters used to evaluate and compare the different simulations are the amine fluxes J_a [g/(m²h)] and the extracted amine fraction E_a [-]. They were both calculated based on the feed side (f) as well as the strip side (s) as follows:

$$E_\mathrm{a}^\mathrm{f} = \frac{\dot{n}_\mathrm{a,in}^\mathrm{f} - \dot{n}_\mathrm{a,out}^\mathrm{f}}{\dot{n}_\mathrm{a,in}^\mathrm{f}} \tag{8}$$

$$E_\mathrm{a}^\mathrm{s} = \frac{\dot{n}_\mathrm{a,out}^\mathrm{s} - \dot{n}_\mathrm{a,in}^\mathrm{s}}{\dot{n}_\mathrm{a,in}^\mathrm{f}} \tag{9}$$

$$J_\mathrm{a}^\mathrm{f} = \frac{\left(\dot{n}_\mathrm{a,in}^\mathrm{f} - \dot{n}_\mathrm{a,out}^\mathrm{f}\right) MW_\mathrm{a}}{A_\mathrm{m}} \tag{10}$$

$$J_\mathrm{a}^\mathrm{s} = \frac{\left(\dot{n}_\mathrm{a,in}^\mathrm{s} - \dot{n}_\mathrm{a,out}^\mathrm{s}\right) MW_\mathrm{a}}{A_\mathrm{m}} \tag{11}$$

Herein, MW_a [g/mol] is the molecular weight of the amine, and A_m [m²] is the membrane area in the module. The extraction is for both sides dependent on the feed concentration. The fluxes are defined positive for an outflow and negative for an inflow of the respective amine from the considered side. This results in a positive feed flux

J_a^f and a negative strip flux J_a^s. Finally, the error e [-] between the feed and the strip values was calculated as follows:

$$e = \text{abs}\left|\frac{x_f - x_s}{\left(\frac{x_f + x_s}{2}\right)}\right| \tag{12}$$

S3.3.2 24-hour analysis

The simulated single pass values are not sufficient for a good comparison with the membrane extraction experiments. Therefore, a 24-hour simulation was made in MATLAB based on the initially collected data. In this simulation, the throughput Q [L/h], initial concentrations $C_{a,0}$ [g/L], and membrane surface A_m [m²] were used in combination with the obtained extracted amine fraction $E_{x,a}$ [-]. Since the extraction fraction can be assumed constant over a changing concentration (see Section 3.3 in the manuscript), it can also be assumed constant over time, resulting in a simplified 24-hour MATLAB simulation. Furthermore, a total extraction time of 24 hours and a total buffer volume of 250 ml were used. The concentration was recalculated 25,000 times (indicated as Θ) resulting in a run-through volume V_θ, which was determined as follows:

$$V_\theta = \frac{Q \cdot t}{\Theta} \tag{13}$$

The mass of extracted amines m_a could then be calculated for each iteration $\theta = 1,2,\ldots,\Theta$, as shown in Equation (14) with $m_{a,\theta=0} = 0$.

$$m_{a,\theta} = m_{a,\theta-1} + C_{a,\theta-1} \cdot V_\theta \cdot E_a \tag{14}$$

Herein, $C_{a,\theta}$ is the concentration of amine a in iteration θ which is recalculated as follows:

$$C_{a,\theta} = \frac{C_{a,\theta-1} \cdot V_{tot} - C_{a,\theta-1} \cdot V_\theta \cdot E_a}{V_{tot}} \tag{15}$$

The overall flux J_a and total extracted amine E_a were then calculated accordingly:

$$J_a = \frac{m_{a,\Theta}}{t \cdot A_m} \tag{16}$$

$$E_a = \frac{m_{a,\Theta}}{C_{a,0} \cdot V_{tot}} \tag{17}$$

The full MATLAB script can be found in Section S4.2.

S3.4 Post-processing

To obtain concentration data from the solved model, the surface averages at both inlets and outlets were monitored. These data were then collected and processed to determine the pH, flux, and extraction of amine a according to the formulas described in Section S3.3. Furthermore, the flow patterns and concentration profiles were studied by visually plotting the results over the mesh nodes, using a colour scale. This visualisation was done using the slice plots for the velocity and a combination of slice and volume plots for the concentration.

S4 MATLAB scripts

This section describes the various MATLAB files used to achieve the required parameters.

S4.1 Equilibrium calculator

To calculate the necessary amounts of chemical compounds to achieve the required buffer solutions, a MATLAB script was written, which could calculate the equilibrium concentrations to use as input for the COMSOL model. To start all variables and constants are defined:

```
syms H3PO4 H2PO4 HPO4 PO4 CO3 HCO3 OH a b c a1 a2 a3

WWH3PO4 = 0.85                  ; %w/w%
DensH3PO4 = 1.685               ; %g/mL of WWH3PO4 solution

MWNa2CO3 = 105.9888;
MWNaHCO3 = 84.007;
MWH3PO4 = 97.994;
MWNaH2PO4 = 119.98;
MWNa2HPO4 = 141.96;
MWNaOH = 39.997;

pKaMBA = 9.4;
pKaIPA = 10.6;
pKaMPPA = 10.0;

MWMBA = 121.18;
MWIPA = 59.11;
MWMPPA = 149.23;

k_H3PO4 = 7.5*10^(-3);
k_H2PO4 = 6.2*10^(-8);
k_HPO4 = 10^(-12);

k_CO3 = 10^(-14)/(4.84*10^(-11));
k_HCO3 = 10^(-14)/(4.16*10^(-7));
```

Next up, the simulation dependent variables such as the pH, buffer capacity and volume, and amine concentration are defined:

```
pH =10.0                        ; % -
```

```
C_Buffer = 0.2              ; % M
V_buffer = 1000             ; % mL
MBA = 1*V_buffer            ; % mg
IPA = 1*V_buffer            ; % mg
MPPA = 1*V_buffer           ; % mg
Va = V_buffer               ; % mL
pHFeed = pH                 ; % -
```

Then, depending on the required pH, the MATLAB script decides on what buffer composition to choose. Furthermore, it calculates the required mass, or volume in case of H_3PO_4, to achieve the requested buffer. These values are printed in grams for the printed parameters ending on "_g" or µL of the predefined 85% H_3PO_4 solution for the printed parameter H3PO4_ww_uL. The equilibrium concentrations are printed in mol/m³, which is the standard unit used in COMSOL. In this code the variables a, b and c describe the number of times a reaction occurs for the buffer compounds.

```
if pH < 5
  h3po4 = H3PO4 - a;
  h2po4 = H2PO4 - b + a;
  hpo4 =  -c + b;
  po4 = c;
  h3o = a+b+c;

  f_H3PO4 = h2po4*h3o/h3po4 == k_H3PO4;
  f_H2PO4 = hpo4*h3o/h2po4 == k_H2PO4;
  f_HPO4 = po4*h3o/hpo4 == k_HPO4;
  f_H3O = h3o == 10^(-pH);
  f_C3 = h3po4 +h2po4 + hpo4 == C_Buffer;

  [H3PO4,H2PO4,  a,b,c]=
    solve([f_H3PO4,f_H2PO4,f_HPO4,f_H3O,f_C3],
      [H3PO4,H2PO4, a,b,c]);

  H3PO4_ww_uL =round((H3PO4*MWH3PO4*V_buffer/1000)/
    DensH3PO4/WWH3PO4*1000,16)
  NaH2PO4_g =round(H2PO4*MWNaH2PO4*V_buffer/1000,16)

  h3po4 =round(1000*(H3PO4 - a),16)
  h2po4 =round(1000*(H2PO4 - b + a),16)
  hpo4 =round(1000*(-c + b),16)
  po4 =round(1000*(c),16)
```

```
  h3o =round(1000*(a+b+c),16)
  oh = round(1000*(10^(-14)/(a+b+c)),16)

elseif pH < 9
  h3po4 =  - a;
  h2po4 = H2PO4 - b + a;
  hpo4 = HPO4 -c + b;
  po4 = c;
  h3o = a+b+c;

  f_H3PO4 = h2po4*h3o/h3po4 == k_H3PO4;
  f_H2PO4 = hpo4*h3o/h2po4 == k_H2PO4;
  f_HPO4 = po4*h3o/hpo4 == k_HPO4;
  f_H3O = h3o == 10^(-pH);
  f_C3 = h3po4 +h2po4 + hpo4 +po4== C_Buffer;

  [H2PO4, HPO4, a,b,c]=
    solve([f_H3PO4,f_H2PO4,f_HPO4,f_H3O,f_C3],
      [H2PO4, HPO4, a,b,c]);

  NaH2PO4_g =round(H2PO4*MWNaH2PO4*V_buffer/1000,16)
  Na2HPO4_g =round(HPO4*MWNa2HPO4*V_buffer/1000,16)

  h3po4 =round(1000*(-a),16)
  h2po4 =round(1000*(H2PO4 - b + a),16)
  hpo4 =round(1000*(HPO4 -c + b),16)
  po4 =round(1000*(c),16)
  h3o =round(1000*(a+b+c),16)
  oh = round(1000*(10^(-14)/(a+b+c)),16)

elseif pH < 11
  h2co3 = a;
  hco3 = HCO3 - a + b;
  co3 = CO3 - b;
  oh = b+a;

  f_CO3 = hco3*oh/co3 == k_CO3;
  f_HCO3 = h2co3*oh/hco3 == k_HCO3;
  f_OH = oh == 10^(-(14-pH));
  f_C10 = h2co3 +hco3 + co3 == C_Buffer;
```

```
  [HCO3, CO3, b,a]=
    solve([f_CO3, f_HCO3, f_OH, f_C10],[HCO3, CO3, b,a]);

  NaHCO3_g =round(HCO3*MWNaHCO3*V_buffer/1000,16)
  Na2CO3_g =round(CO3*MWNa2CO3*V_buffer/1000,16)

  h2co3 =round(1000*(a),16)
  hco3 =round(1000*(HCO3 - a + b),16)
  co3 =round(1000*(CO3 - b),16)
  oh = round(1000*(b+a),16)
  h3o = round(1000*(10^(-14)/(b+a)),16)

else
  h3po4 =  - a;
  h2po4 = H2PO4 - b + a;
  hpo4 = HPO4-c + b;
  po4 = c;
  oh =OH -( a+b+c);

  f_H3PO4 = h2po4/h3po4/oh == k_H3PO4/10^(-14);
  f_H2PO4 = hpo4/oh/h2po4 == k_H2PO4/10^(-14);
  f_HPO4 = po4/oh/hpo4 == k_HPO4/10^(-14);
  f_OH = oh == 10^(-14+pH);
  f_C3 = h3po4 +h2po4 + hpo4 +po4 == C_Buffer;

  [H2PO4, OH, a,b,c]=
    solve([f_H3PO4,f_H2PO4,f_HPO4,f_OH,f_C3],[H2PO4, OH, a,b,c]);

  NaH2PO4_g =round(H2PO4*MWNaH2PO4*V_buffer/1000,16)
  NaOH_g =round(OH*MWNaOH*V_buffer/1000,16)
  Na2HPO4_g =round(HPO4*MWNa2HPO4*V_buffer/1000,16)

  h3po4 =round(1000*(-a),16)
  h2po4 =round(1000*(H2PO4 - b + a),16)
  hpo4 =round(1000*(HPO4-c + b),16)
  po4 =round(1000*(c),16)
  oh =round(1000*(OH-(a+b+c)),16)
  h3o = round(1000*(10^(-14)/(OH-( a+b+c))),16)
```

```
end
```

Finally, the amine equilibrium is determined. Herein $a1$, $a2$ and $a3$ describe the number of times the protonation reaction occurs for the amines with pKa 9.4, 10.0, and 10.6, respectively. These are also given in mol/m^3.

```
MBA = MBA/MWMBA/Va;
IPA = IPA/MWIPA/Va;
MPPA = MPPA/MWMPPA/Va;
H3O = 10^(-pHFeed);

mbah =round( solve(H3O*(MBA-a1)/a1 == 10^(-pKaMBA), a1), 10);
mba = MBA - mbah;
ipah =round( solve(H3O*(IPA-a2)/a2 == 10^(-pKaIPA), a2), 10);
ipa = IPA - ipah;
mppah =round( solve(H3O*(MPPA-a3)/a3 == 10^(-pKaMPPA), a3), 10);
mppa = MPPA - mppah;

mba = mba *1000
mbah = mbah *1000
ipa = ipa * 1000
ipah = ipah * 1000
mppa = mppa * 1000
mppah = mppah * 1000
```

The buffer capacity calculations were also adjusted to exclude "po4" and "co3" when adjusting the pH. This way, the capacity to protonate the amines upon their addition to the buffer solution remained constant, as this was concluded to have the biggest impact on the pH.

S4.2 24-hour approximation

The second MATLAB script approximated the 24-hour membrane extraction experiments, using the results of the one run-through simulations in COMSOL. Within this simulation, the variables such as the throughput, initial concentration of amines and one run-through extraction are imported from Microsoft Excel, in which every row gives the post-processing of a different simulation.

```
Q=xlsread("COMSOL_results.xlsx", 'AV7:AV150')
C = xlsread("COMSOL_results.xlsx",'E7:F150')
EXTR = xlsread("COMSOL_results.xlsx",'BM7:BR150')
```

The throughput, defined as "Q", is immediately imported correctly in L/h. The concentration import reads the amount of mol/m³ of pKa 9.4 in both unprotonated and protonated form. Since the initial concentration of all amines is equal for all experiments these can be determined as follows:

```
CONC0 =(C(:,1)+C(:,2))*121.180000000/1000;
CONC_MBA = CONC0;
CONC_MPPA = CONC0;
CONC_IPA = CONC0;
```

The one run-through extraction is amine-dependent and is averaged over the feed and strip side:

```
EXTR_MBA =(EXTR(:,1)+EXTR(:,4))/2;
EXTR_MPPA = (EXTR(:,2)+EXTR(:,5))/2;
EXTR_IPA = (EXTR(:,3)+EXTR(:,6))/2;
```

For continuation of the calculation, some parameters are needed, namely the total liquid volume on the strip side, the number of hours, the number of times the concentration has to be recalculated, and the membrane area.

```
TOT_VOL = 0.25000000                  ; %(L)
TIME = 24                             ; %(hr)
tot_runthrough = 25000;
MEMB = 0.00056030000                  ; %(m^2)
```

The number of iterations splits the volume according to the flow rate as follows:

```
MODULE_VOL = Q*TIME/tot_runthrough
```

Then, the amount of mass extracted is iterated for each amine. To achieve an initial zero-matrix of the required length the calculation Q-Q is used.

```
GRAM_MBA = Q-Q;
GRAM_MPPA = GRAM_MBA;
GRAM_IPA = GRAM_MBA;

for n = 1:tot_runthrough
  GRAM_MBA=GRAM_MBA+MODULE_VOL.*CONC_MBA.*EXTR_MBA;
  CONC_MBA = (MODULE_VOL.*CONC_MBA.*(1-EXTR_MBA) +
    (TOT_VOL-MODULE_VOL).*CONC_MBA) /TOT_VOL;

  GRAM_MPPA=GRAM_MPPA+MODULE_VOL.*CONC_MPPA.*EXTR_MPPA;
  CONC_MPPA =(MODULE_VOL.*CONC_MPPA.*(1-EXTR_MPPA) +
```

```
    (TOT_VOL-MODULE_VOL).*CONC_MPPA) /TOT_VOL;

  GRAM_IPA=GRAM_IPA+MODULE_VOL.*CONC_IPA.*EXTR_IPA;
  CONC_IPA = (MODULE_VOL.*CONC_IPA.*(1-EXTR_IPA) +
    (TOT_VOL-MODULE_VOL).*CONC_IPA) /TOT_VOL;
end
```

The resulting vectors are used to calculate the overall extractions E_a and fluxes J_a. These results are written into the initial Microsoft Excel file for easy comparison to the benchmark experiment.

```
FLUX_MBA = GRAM_MBA/TIME/MEMB
FLUX_MPPA = GRAM_MPPA/TIME/MEMB
FLUX_IPA = GRAM_IPA/TIME/MEMB

TOT_EXTRACT_MBA = GRAM_MBA ./ (CONC0*TOT_VOL)
TOT_EXTRACT_MPPA = GRAM_MPPA ./ (CONC0*TOT_VOL)
TOT_EXTRACT_IPA = GRAM_IPA ./ (CONC0*TOT_VOL)

result=[GRAM_MBA, GRAM_MPPA, GRAM_IPA, CONC_MBA, CONC_MPPA, CONC_IPA,
 TOT_EXTRACT_MBA, TOT_EXTRACT_MPPA, TOT_EXTRACT_IPA,  FLUX_MPPA,
 FLUX_MBA,FLUX_IPA]

writematrix(result,"COMSOL_results.xlsx","Range",'CF7:CQ150')
```

S5 Robustness study

S5.1 Effect of mesh size

The mesh was created using the same steps and parameters as explained in Section S3.2.4, except for the mesh sizes. The general mesh size and mesh size of the buffer domains were adjusted to be a fluid dynamics fine mesh, whilst the buffer boundaries were chosen as a fluid dynamics finer mesh. This combination resulted in the domain elements and degrees of freedom as shown in Table S7.

Table S7. Elements and DOFs achieved for the standard and finer mesh sizes of the flat sheet module.

	Coarser	Finer
Domain elements	227,629	639,546
Boundary elements	31,714	74,154
DOF solved for	1,701,047	4,436,173
Internal DOF solved for	378,780	848,805

The fluxes and solute recoveries of the flat sheet module for a varying mesh size are given in Figure S3. The variations had a relative error not exceeding -2.0 %, while there was no difference in the pH values. Therefore, it can be concluded that the normal mesh size used in further simulations gave a sufficiently accurate and precise result.

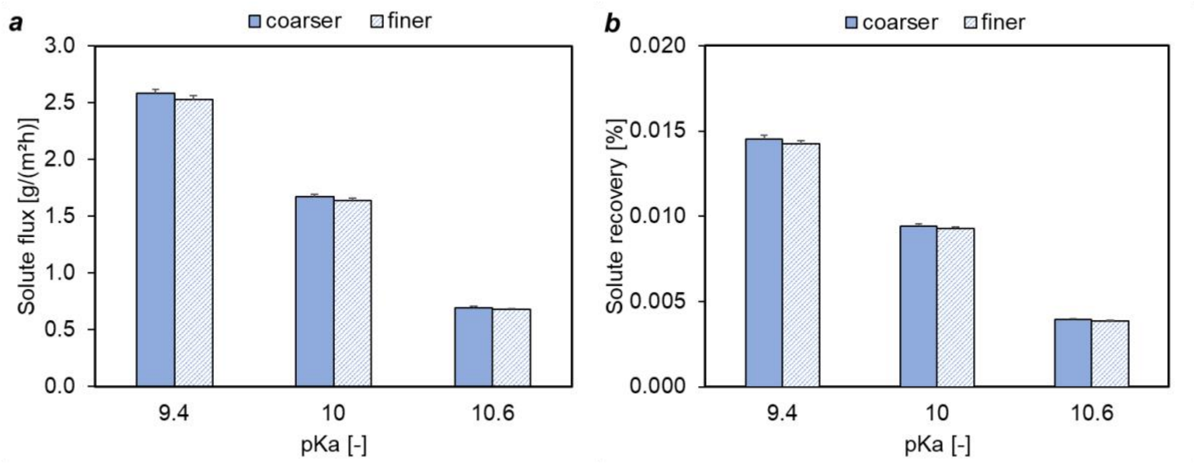

Figure S3. Simulated influence of the mesh size on (a) the solute flux, and (b) the solute recovery for a single pass through the flat sheet module.

S5.2 Boundary conditions

The standard model employs the pressure outlet condition with suppressed backflow for the “Turbulent Flow” physics. For the simulation of the concentrations, the reaction equilibria are made at the inlet boundaries. The standard model was altered in three different ways: (1) using a velocity outlet condition, (2) enabling backflow, and (3) not calculating the reaction equilibria. These adjustments give a negligible change of outflow results for the flat sheet module (not exceeding -0.2 %). Therefore, it can be concluded that the impact of these boundary conditions is minimal on the tested simulation.

S6 Effect of flow conditions and membrane properties

S6.1 Effect of the buffer diffusion coefficients

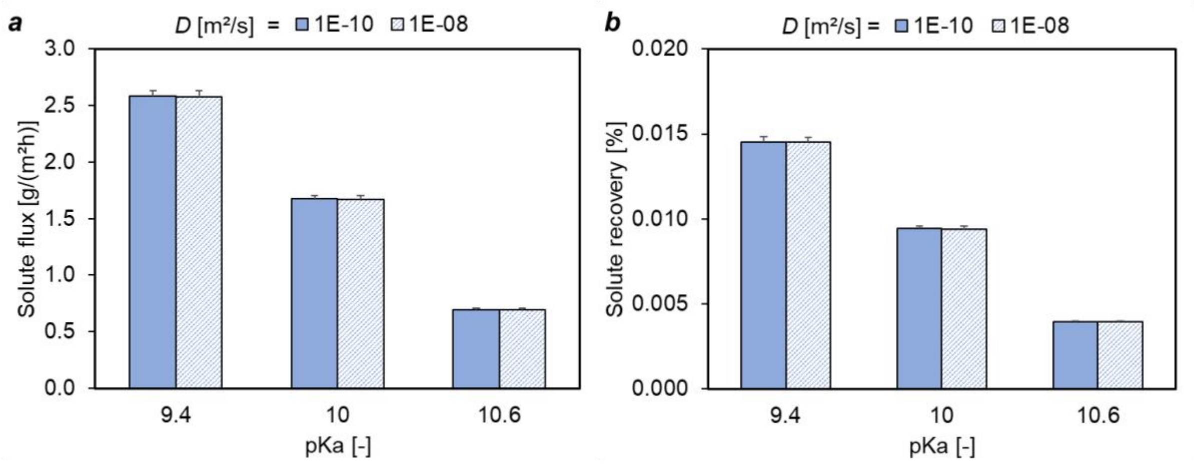

Figure S4. Simulated influence of the diffusion coefficient in the buffer solutions on (a) the solute flux, and (b) the solute recovery for a single pass through the flat sheet module.

S6.2 Effect of the membrane porosity

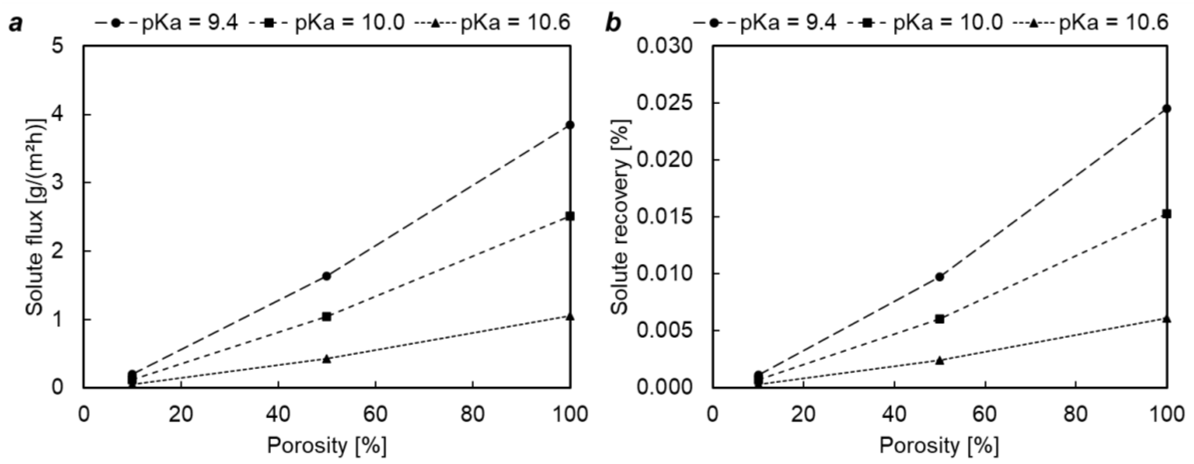

Figure S5. Simulated influence of the membrane porosity on (a) the solute flux, and (b) the solute recovery for a single pass through the flat sheet module.

S6.3 Effect of the membrane permeability

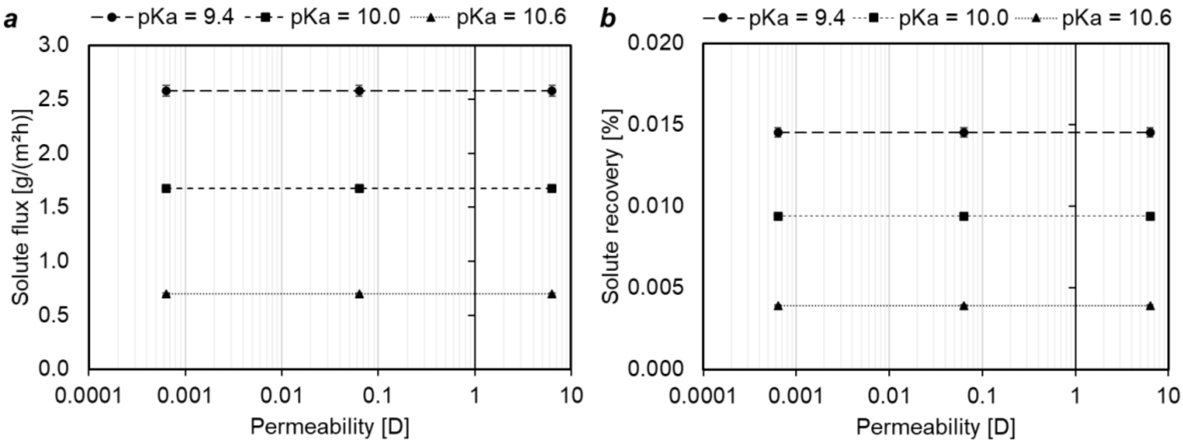

Figure S6. Simulated influence of the membrane permeability on (a) the solute flux, and (b) the solute recovery for a single pass through the flat sheet module.

S6.4 Effect of the membrane diffusion coefficient

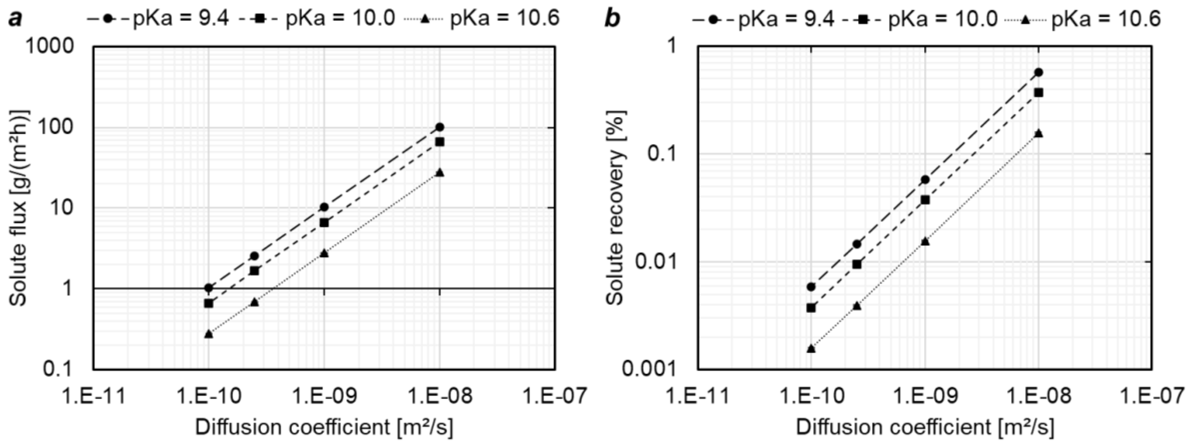

Figure S7. Simulated influence of the membrane diffusion coefficient on (a) the solute flux, and (b) the solute recovery for a single pass through the flat sheet module.

S7 Diffusion coefficients as a function of temperature

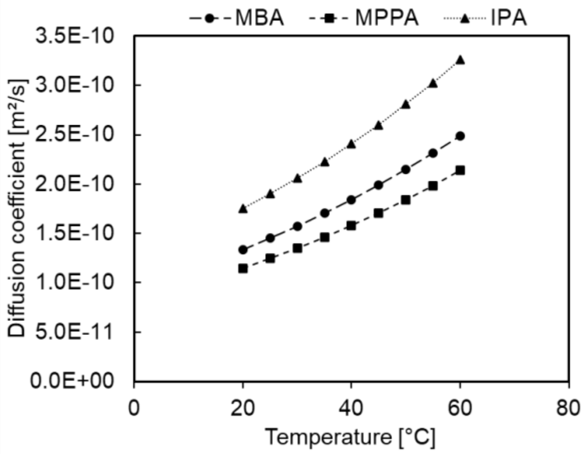

Figure S8. Simulated diffusion coefficients of the target solutes in the ionic liquid [$P_{6,6,6,14}$][$N(Tf)_2$] as a function of the temperature, obtained from COSMO-RS.

S8 Model validation

Table S8. Root Mean Squared Error (RMSE) of the solute flux and the solute recovery for the different solutes at all the considered conditions.

		RMSE of solute flux			RMSE of solute recovery		
		MBA	MPPA	IPA	MBA	MPPA	IPA
F [L/h]	5	0.95	0.33	0.13	1.47	4.53	1.17
	7.5	0.40	0.05	0.06	3.24	5.71	0.85
	10	0.37	0.48	0.35	4.82	5.77	2.29
C [g/L]	0.5	0.29	0.47	0.64	3.25	6.44	5.72
	1	0.18	0.48	0.35	4.82	5.77	2.29
	2.5	0.78	1.43	3.41	3.46	6.71	7.05
pH [-]	9	0.24	0.44	2.09	3.93	5.03	8.62
	9.5	0.45	0.91	0.25	1.38	2.57	1.49
	10	0.18	0.48	0.36	4.82	5.74	2.28
	10.5	1.00	2.60	1.01	8.51	16.01	5.25
	11	10.22	11.37	2.31	51.47	51.13	6.81

S9 Effect of process conditions

S9.1 Effect of the strip side concentration

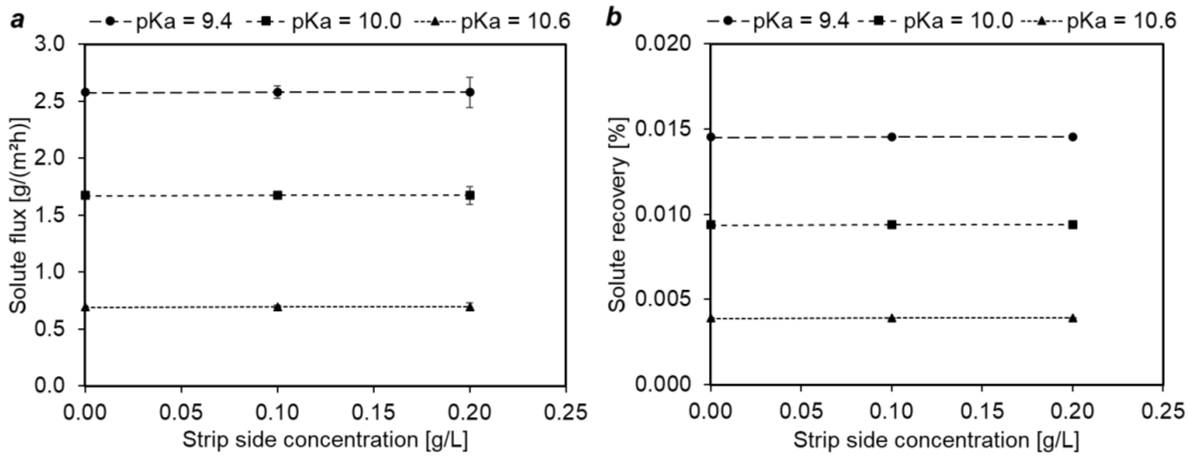

Figure S9. Simulated influence of the strip side concentration on (a) the solute flux, and (b) the solute recovery for a single pass through the flat sheet module.

S9.2 Protonation kinetics in the strip

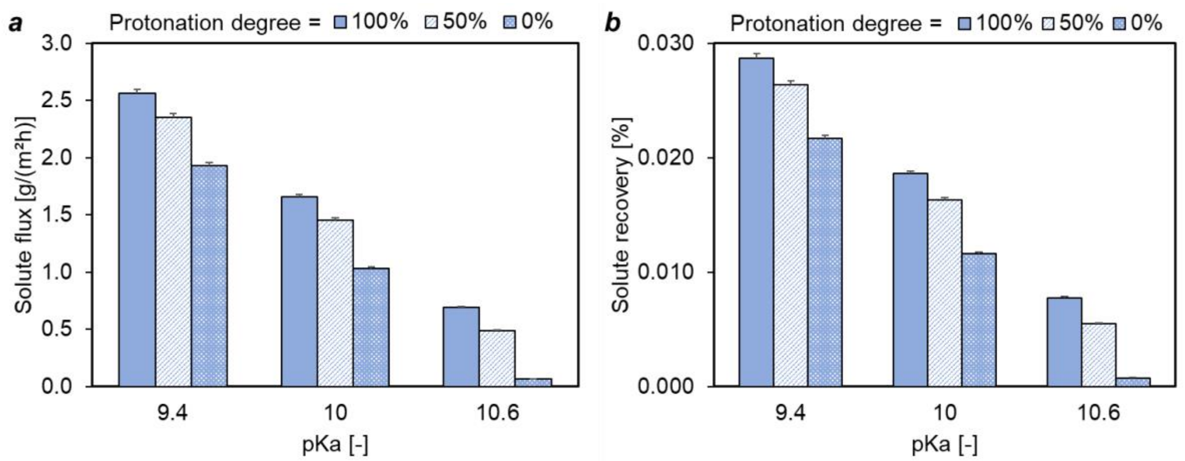

Figure S10. Simulated effects of protonation kinetics at the strip side on (a) the solute flux, and (b) the solute recovery in the flat sheet module for a single pass through the module. The strip concentration was 0.2 g/L and the buffer flow rates were 5 L/h.

S9.3 Effect of the strip pH

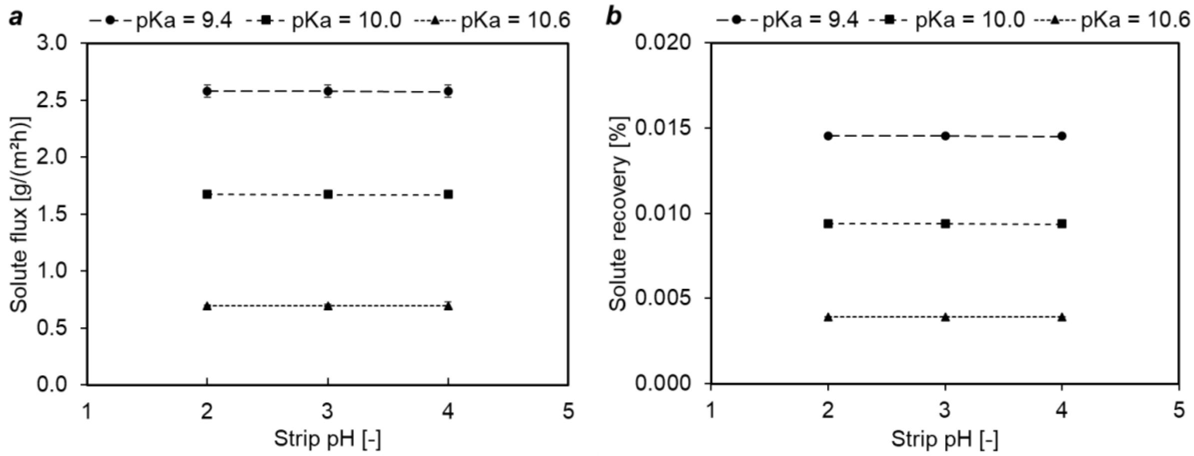

Figure S11. Simulated influence of the strip side pH on (a) the solute flux, and (b) the solute recovery for a single pass through the flat sheet module.

S10 Statistical analysis

Table S9. Comparison of solute flux and recovery data across different flow rates. The standard conditions are highlighted in bold and yellow. Results are based on an independent samples t-test with unequal variances. p < 0.05 indicates statistical significance (*).

	MBA			MPPA			IPA		
F [L/h]	5	7.5	**10**	5	7.5	**10**	5	7.5	**10**
J_1	1.20	2.07	**2.89**	3.60	4.72	**5.87**	0.75	0.70	**0.47**
J_2	1.39	1.91	**2.05**	4.20	4.64	**5.17**	0.53	0.82	**1.31**
J_3			**2.24**			**5.37**			**0.76**
p-value	0.038*	0.250		0.053	0.059		0.506	0.772	
R_1	10.04	16.17	**19.98**	23.58	30.60	**35.99**	4.71	4.69	**2.76**
R_2	12.26	15.92	**16.49**	27.80	30.85	**31.27**	3.05	4.93	**8.20**
R_3			**17.12**			**30.46**			**4.51**
p-value	0.030*	0.231		0.112	0.395		0.535	0.852	

Table S10. Comparison of solute flux and recovery data across different feed concentrations. The standard conditions are highlighted in bold and yellow. Results are based on an independent samples t-test with unequal variances. p < 0.05 indicates statistical significance (*).

	MBA			MPPA			IPA		
C [g/L]	0.5	**1**	2.5	0.5	**1**	2.5	0.5	**1**	2.5
J_1	0.77	**2.67**	5.93	1.85	**5.87**	13.51	0.10	**0.47**	5.33
J_2	0.90	**2.46**	4.88	2.06	**5.17**	10.83	0.32	**1.31**	5.19
J_3	1.37	**2.71**		2.89	**5.37**		1.40	**0.76**	
p-value	0.006*		0.112	0.002*		0.119	0.643		0.002*
R_1	13.13	**19.98**	17.47	25.06	**35.99**	34.51	1.44	**2.76**	11.69
R_2	15.32	**16.49**	11.32	28.08	**31.27**	26.16	4.52	**8.20**	10.32
R_3	17.16	**17.12**		32.60	**30.46**		13.01	**4.51**	
p-value	0.169		0.451	0.229		0.689	0.781		0.054

Table S11. Comparison of solute flux and recovery data across different feed pH values. The standard conditions are highlighted in bold and yellow. Results are based on an independent samples t-test with unequal variances. $p < 0.05$ indicates statistical significance (*).

	MBA					MPPA					IPA				
pH	9	9.5	**10**	10.5	11	9	9.5	**10**	10.5	11	9	9.5	**10**	10.5	11
J_1	1.41	1.70	**2.67**	3.51	10.28	1.95	2.81	**5.87**	8.41	13.50	1.54	0.31	**0.47**	0.46	1.74
J_2	1.10	1.38	**2.46**	3.68	11.47	1.57	2.29	**5.17**	8.70	14.83	2.30	0.81	**1.31**	0.49	6.32
J_3	1.77		**2.71**		10.42	2.49		**5.37**		14.70	2.84		**0.76**		0.27
J_4	1.53				18.32	2.13				26.94					1.97
J_5					12.04					15.26					
p-value	0.001*	0.050		0.006*	0.003*	0.000*	0.009*		0.001*	0.009*	0.046*	0.488		0.275	0.278
R_1	11.85	12.51	**19.98**	22.15	65.38	14.55	17.89	**35.99**	47.50	81.74	5.18	1.79	**2.76**	2.65	6.28
R_2	7.16	10.40	**16.49**	22.79	75.03	9.60	14.76	**31.27**	48.67	93.32	7.30	4.71	**8.20**	2.84	16.22
R_3	13.36		**17.12**		63.22	16.56		**30.46**			0.16		**4.51**		1.62
R_4	11.49				72.20	14.13					16.29				13.33
R_5															0.14
p-value	0.010*	0.029*		0.042*	0.000*	0.001*	0.007*		0.007*	0.049*	0.606	0.448		0.272	0.531

References

[1] D.J. Glatz, B. Cross, Reactions and separations: Optimal design of a liquid-liquid extraction system, Chem Eng Prog, (2021) 22–27.

[2] R. Wu, Y. Tan, F. Meng, Y. Zhang, Y.X. Huang, PVDF/MAF-4 composite membrane for high flux and scaling-resistant membrane distillation, Desalination, 540 (2022) 116013.

[3] G. Van Eygen, D. Mariën, A. Vananroye, C. Clasen, B. Van der Bruggen, A. Buekenhoudt, J.A.P. Coutinho, P. Luis, Facilitated solvent screening for membrane-based extraction of chiral amines via a priori simulations, J Mol Liq, 375 (2023) 121351.

[4] ChemBK, ChemBK Database, (n.d.).

[5] V.S.P. V. Alluri, Measurement and Prediction of pKa of Linear and Cyclic Amines Using Group-Additivity and Artificial Neural Network (ANN) Models, University of Regina, 2022.

[6] FooDB, FooDB Database, (n.d.).

[7] “National Center for Biotechnology Information,” PubChem, (n.d.).

[8] I. Smets, P. Van Puyvelde, Algemene en Technische Scheikunde, (2021).

[9] C.C. Ho, A.L. Zydney, Measurement of membrane pore interconnectivity, J Memb Sci, 170 (2000) 101–112.

[10] J. Zhang, J. De Li, S. Gray, Effect of applied pressure on performance of PTFE membrane in DCMD, J Memb Sci, 369 (2011) 514–525.

[11] COMSOL, COMSOL Documentation, (n.d.).

[12] COMSOL Support, COMSOL Support - Knowledge Base, (n.d.).